Simulation Study on Determination of Gas-Liquid Profile in an Aeration Tank for Mixing Process by using an Electrical Capacitance Tomography System

Nur Tantiyani Ali Othman[1*], Muhammad Danial Najmi Ronizan[2]

[1*,2]Department of Chemical and Process Engineering, Faculty of Engineering and Built Environment, Universiti Kebangsaan Malaysia, 43600, Bangi UKM, Selangor.

Corresponding author* email: tantiyani@ukm.edu.my
Accepted 3 March 2021, available online 31 March 2021

ABSTRACT

As an electrical capacitance tomography (ECT) is a non-intrusive and non-invasive technique, it has been used a lot in industrial applications such as fluidized beds, palm oil processing industry, gas/solids cyclones and oil and gas industry. It was found that the developing process of the ECT hardware takes a longer time and it requires specialized technical skills to design it. Thus, a simulation technique was studied as it can be executed in a short period of time as compared to the experimental approach. In this study, 3D ECT model system was developed using COMSOL® Multiphysics software where the sensors consist of 16 electrodes allocated around the outer layer of the tank with a diameter of 110 mm and height of 180 mm. To observe a flow pattern and gas hold-up in the gas-liquid multiphase flow, three parameters were manipulated; the feed of a hot air velocity that range of 0.01-0.1 ms^{-1}, types of inlet gas (carbon dioxide gas, oxygen gas and hydrogen gas) and an electrical charge voltage ranging from 1-15V. The simulation results show that the average velocity increased as the feed of the hot air was increased. Besides, the lowest value of the gas hold-up was observed as the hydrogen gas was used as the feed, meanwhile there was no noticeable difference between carbon dioxide and oxygen gas due to a lower gas density. In addition, no significant difference was indicated when the electrode was charged at different voltage of 1V, 5V and 15V. From these results, the optimum condition for average velocity and gas hold-up was determined that can be used to develop the ECT model in the future for mixing process purpose.

Keywords: Electrical Capacitance Tomography, Gas-Liquid Flow, COMSOL®, Velocity, Aeration Tank

1. Introduction

Since 1970s, tomography was extended applied in a medical field for diagnostic purposes, for example, X-rays are using radiation sources to see inside a human's body such as bone without doing any operation. Also, the application of the tomography was widely used in the industrial process, such as gamma-ray, electrical resistance tomography (ERT), electrical impedance tomography (EIT), electromagnetic tomography (EMT) and electrical capacitance tomography (ECT) for observe two-phase flow inside the system [1]. It is an essential and required that it is able to visualize the flows in a real-time to understand the multiphase flow interactions. As the data gained can benefit in the process of equipment designing, process control and monitoring the entire process [2]. However, direct measurement of a multiphase flow profile and concentration distribution inside the system/pipeline is quite challenging by the traditional experimental observation. Therefore, an industrial process tomography has been developed to visualize the internal behavior of the industrial processes by providing the cross-sectional images on the flow inside a pipeline or vessel without disturbing the entire flow process [3].

Amongst all the process tomography techniques, recently, the prominence of the ECT application in the industrial processes retains growing. By using ECT, the flow regime and the degree of entrainment can be identified, as well determine the flow rate distribution accurately. Besides, ECT can provide details information about the content inside the vessel based on the dielectric properties of the flowing materials without any disturbance of the flow system [4]. Mostly, ECT has higher temporal resolution as compared to the conventional X-ray tomography in order to observe and

estimate prompt variations in a hydrodynamic behavior [5]. This ECT technique is non-invasive, non-intrusive, non-destructive, fast imaging speed, no radiation and flexible sensor that can fit around virtually to any vessel geometry such as no straight cylindrical vessel, T-junctions and L-junctions that shown the ECT technique is better than others tomography systems such as EMT and ERT [6]. It is because, for the EMT system, industrial sensors need extensive screening to ensure enough signal to reduce a noise ratio and compliance with some international electromagnetic compatibility standards. Meanwhile, the magnetic screening is difficult to implement in the industry as practically, it is more expensive and due to the manufacturing restrictions issue on a single EMT that may restraint only to the industrial applications for a small scale used [7]. For the ERT, the front-end signal processing circuit converts a resistance to a voltage, while in the ECT, it converts a capacitance to a voltage.

Generally, a topology of the ECT system consists of the ECT sensor which made up of 8 to 16 electrodes, signal conditioning circuits, central control units and a personal computer (PC). The electrode is made up of conductive plates such as copper worked as a sensing surface that contacts directly with the vessels that wanted to be measured. The signal conditioning circuit used to gather data and transform it into a digital. A central control unit used to synchronize all the processes and send the data back to the PC. The PC then obtain the measurement reading, save the data, recreate images from integral measurements and take action feedback to regulate the flow inside the vessel [4]. The multi-electrode sensor measured the deviations in the capacitance and then recreate a permittivity distribution using the obtained capacitance data. The measurement of capacitance is determined by equation (1) where C is a capacitance, $\mathcal{E}_0$ is a permittivity of free space, $\mathcal{E}_r$ is the permittivity of the dielectric, A is the area of the plate and d_p is the distance between those plates. The $\mathcal{E}_0$ and $\mathcal{E}_r$ are the global average of the fluid dielectric property over the entire permittivity. If the distance between plates and the area of the plates are known, by measuring capacitance, the dielectric constant can be measured directly as the capacitance is proportional to the permittivity between the electrodes.

$$C = \frac{\varepsilon_0 \varepsilon_r A}{d_p} \tag{1}$$

If the first electrode is assigned as the source of the electrode, then the rest of the electrodes will act as the detector electrodes. The detector electrodes are connected to the virtual ground terminals, so that it will remain at a zero potential with respect to a ground. Then, the capacitance between first electrode and other electrodes will be measured. After that, second electrode will be assigned as the source electrode and the measurement process is repeated. The whole cycle of an exciting electrode and measuring the subsequent inter-electrode capacitances will be repeated. Pendelton et al. conducted a research to visualize two-phase gas-liquid pipe flows using ECT [8]. They studied a numerical comparison between the gamma-ray densitometer with the ECT system and found that the dominant structure is a slug flow when the superficial gas velocities are 0.2-12.0 ms^{-1} and the superficial oil velocities are 0.05-1.0 ms^{-1}. Besides, they found that these two techniques have a good agreement in a case of a stratified and coherent slug flow. While, Mohamad et al. applied the ECT system to observe materials distributions in the pipelines conveying crude palm oil [2]. They concluded that ECT is able to observe the liquid's composition that existed in the vessel in order to design and develop enhanced process equipment in the mill processes.

Yet, the process of developing the ECT model experimentally will take a longer time and it requires specialized technical skills to design it. As simpler besides to save more time, the simulation technique was approached. One of the simulation software which is COMSOL® Multiphysics has been offered an integration development environment to the users for chemical, fluid, mechanical and electrical applications. Also, COMSOL® Multiphysics using finite element method where it can be connected with others software such as MATLAB©, SolidWorks© and DesignModeler©. Thus, the simulation study is preferred as this approach is much easier, besides save much time in order to develop ECT system as compared to the hardware development. From the simulation studied, the information such as a gas-liquid flow regime, flow velocity, flow composition distribution and else can be obtained that can be used to develop for a real situation in a process control and monitoring flow in the industry.

Hence, in this study, the ECT system model was developed using an AutoCAD® and COMSOL® Multiphysics software to simulate the flow pattern of gas-liquid phase inside the aeration tank. The variations parameter of a velocity of inlet gas, three types of inlet gases and charge of electrodes voltage have been studied to determine the optimum condition for gas-liquid phase flow in the aeration tank ECT system for a mixing process purpose.

2. Methodology

The standard procedure for simulation studied is shown as Figure 1 where generally it has seven steps including selection of the related physics module, development of the geometry model, define material properties and boundary conditions, generating meshing, perform the simulation and finally utilize the post-processing capabilities to inspect the

parameters. In this study, three-dimensional space was selected and a model of bubbly flow (laminar flow) and electrostatic are preferred as these models are more suitable for gas bubbles in the gas-liquid phase with dielectric materials. Then, the ECT model was developed using AutoCAD® 2020 before it being exported to the COMSOL® interphase.

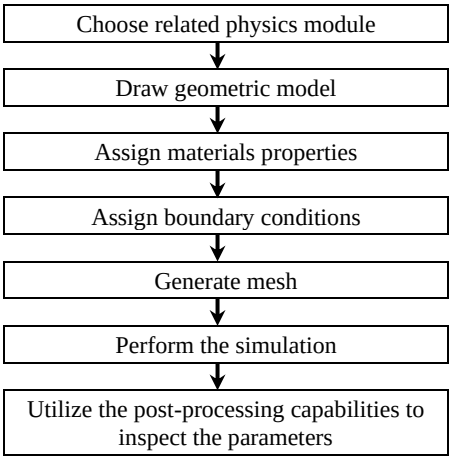

Figure. 1. Flowchart for simulation methodology

Figure 2 shows the 3D ECT model with details configuration and dimension on a side view (left figure) and top view (below). It has 16 number of electrodes sensor that mounted equally with a 22.5^0 angle for each of them with the length of the electrode is 18 mm. The electrodes attached to a tank with an outer tank diameter of 110 mm, height of tank is 180 mm and the wall thickness is 5 mm.

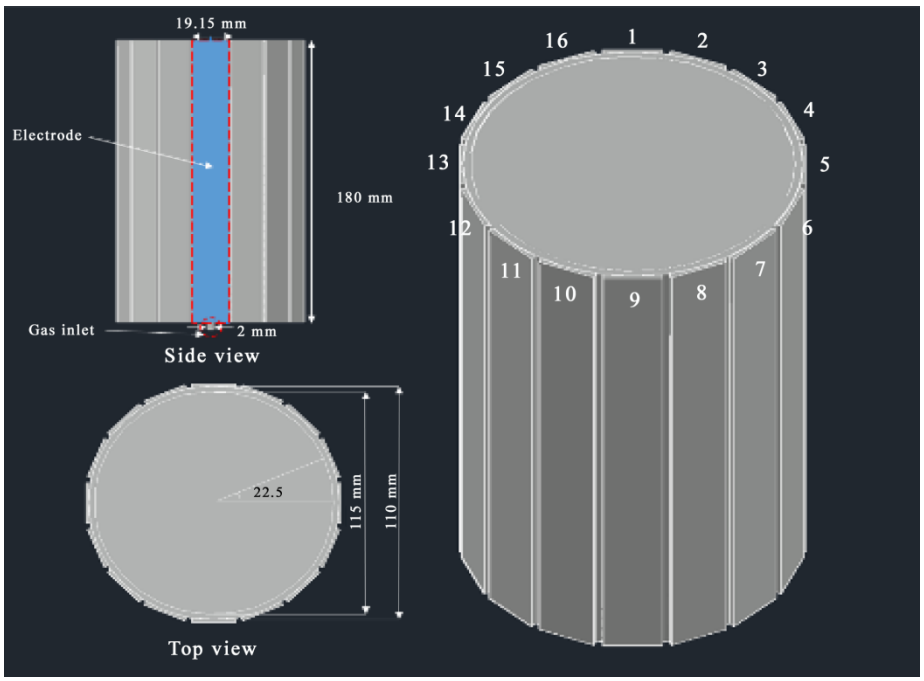

Figure. 2. The configuration of the ECT model developed by AutoCAD®

In this study, a tap water, carbon dioxide gas, oxygen gas and hydrogen gas are used as the fluid flowing inside the ECT system and the details material's properties are shown in Table 1 [9]. To start the simulation process, the boundary conditions are defined as an exciting electrode's potential is set as V_0, meanwhile the remaining of the detecting electrodes are set at ground potential at 0V. For example, when the first electrode becomes the exciting electrode at 1V, the others electrodes will become detecting electrodes that remained at the ground potential which is 0V. Besides, the hot air inlet is supplied at the bottom of the tank whereas the water remained inside the tank.

Table 1. Materials properties

Properties	Water	Carbon dioxide	Oxygen	Hydrogen
Density, ρ (kgm^{-3})	997	1.98	1.45	0.0898
Dielectric permittivity, ε_r	80.0	1.6	1.85	1.0

Firstly, the effect of a hot air velocity on the gas-liquid phase inside the tank was studied. The variation of the air velocity was changed between 0.01-0.1 ms-1, meanwhile the type of gas was fixed which is a carbon dioxide gas feed. Next, the various type of gas was supplied where the oxygen gas and hydrogen gas were feed into the tank with the inlet velocity is fixed at 0.1 ms^{-1}. Finally, the initial voltage charged at the electrode was manipulated between 1-15V. The next step is meshing process where the meshed tank was generated with a finer element size using a meshing builder as shown in Figure 3. Figure 3 (a) shows the top view and Figure 3 (b) shows the overall 3D view of the ECT tank model after meshing process.

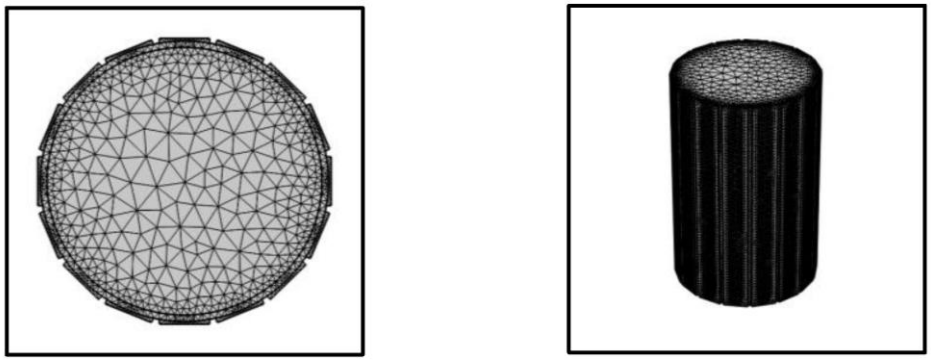

(a) (b)

Figure. 3. a) Top view of ECT and (b) overall 3D view of ECT tank model after meshing process

3. Results and Discussions

3.1 Flow Pattern of Gas-Liquid Phase inside a Tank at Different Inlet Gas Velocity

The inlet gas velocity was changed at v=0.01, 0.05 and to 0.1 ms^{-1} with the gas supplied is a carbon dioxide gas. Figure 4 shows the average of the water velocity inside the tank at different inlet of the gas velocity. It shows the similar pattern trend for the water velocity for all different velocities, where it is increases as the inlet of gas velocity is increases where the highest water velocity is shown at v=0.1 ms^{-1}. Besides, it can be observed that the water velocity inside the tank becomes stable after 30 s for v=0.1 ms^{-1} and after 40 s for v= 0.05 ms^{-1} due to the rate of the water turbulence has been stabilized over the processing time (Tao F. et al., 2019). However, the water velocity inside the tank remained unstable even after 60 seconds for v= 0.01 ms^{-1} due to lower water pressure.

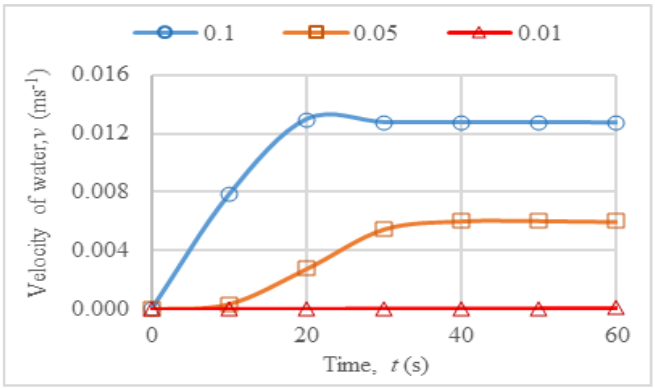

Figure. 4. The velocity of water inside the tank when the inlet velocity of the gas changes

Figure 5 shows the flow profile of the water streamline inside the tank within t=60 s at three different of the inlet gas velocities; at v=0.01, 0.05 and 0.1 ms^{-1} with the arrow at the streamline shows the flow direction. The bar contour color shows the average velocity inside the tank where the dark blue color shows the lowest velocity; 0 ms^{-1}, and the red color shows the highest velocity; 0.1 ms^{-1}. It shows in the case of v=0.01 ms^{-1}, the level of the streamline is quite low where the movement of the water streamline only at the one-third of the tank's height. As the inlet gas velocity is quite low and it don't have enough momentum to hold up and ensure the water to flow throughout liquid-gas multiphase flow in the entire tank. In the case of v=0.05 ms^{-1}, the pattern of the water streamline moved a little bit higher as compared to v=0.01 ms^{-1}, where the distribution of the streamline moved almost the entire of the tank at t=60 s. Meanwhile, in the case of v=0.1 ms^{-1}, the streamline is quite high at the beginning as compared to the others where the flow distribution of the water streamline moved throughout of the entire tank become faster only after t=30 s. It is because when the inlet gas velocity is increases, the gas holdup and the water turbulence inside the tank also increases causing the movement of the water streamline flow throughout the entire tank where the variances in the inlet gas velocity also affected the gas holdup inside the tank.

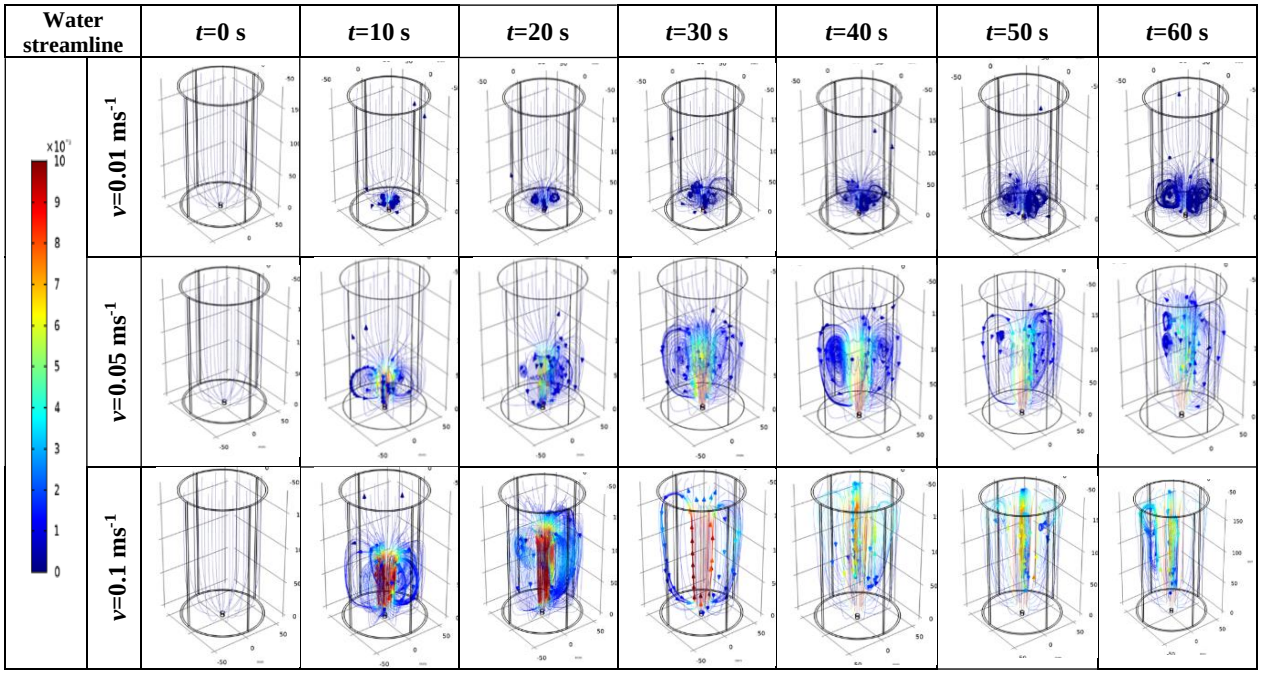

Figure. 5. The water streamlines inside the tank between t=0-60 s at different inlet gas velocity v=0.01, 0.05 and 0.1 ms^{-1}

Figure 6 shows the gas holdup inside the tank at different inlet of the gas velocity where the highest gas holdup is shown at v=0.1 ms^{-1}, whereas the lowest is at v=0.01 ms^{-1} which is unseen in the graph due to low velocity. It shows the inlet gas velocity was affected the gas holdup inside the tank where it is increases as the gas increases due to the turbulence of water inside the tank increases as the inlet gas velocity is increases causing the gas holdup increases [10].

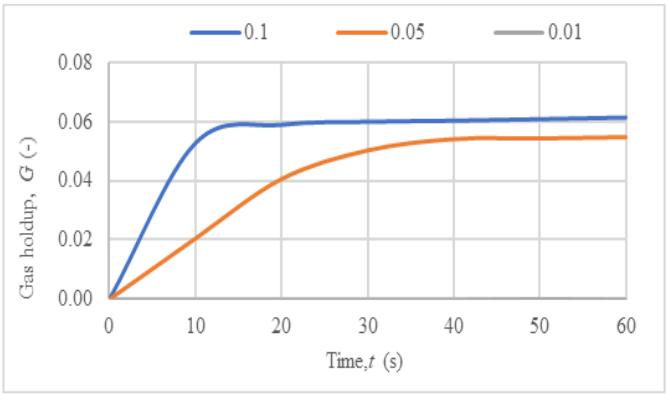

Figure. 6. The gas holdup inside the tank at different inlet of the gas velocity

where the highest gas holdup is at v=0.1 ms^{-1}

Figure 7 shows the formation of gas holdup inside the tank within t=60 s at three different of the inlet gas velocities; v=0.01, 0.05 and 0.1 ms^{-1}. The gas holdup was observed based on the gas volume fraction in the liquid-gas phase flow inside the tank. The bar contour color shows the gas holdup inside the tank where the dark blue color shows the lowest gas holdup; 0, while the red color shows the highest gas holdup; 0.2. It was observed at t=30 s, in the case of v=0.01 ms^{-1}, the formation of the gas holdup is only shown at one-third of the tank's height. Meanwhile, in the case of v=0.05 ms^{-1}, at t=30 s, the formation of the gas holdup formed almost in the half of the tank for v=0.05 ms^{-1}, and it almost cover the entire of the tank in the case of v=0.1 ms^{-1}. Also, the formation of the gas holdup throughout the entire tank become faster after t=30 s for v=0.1 ms^{-1} as compared to others.

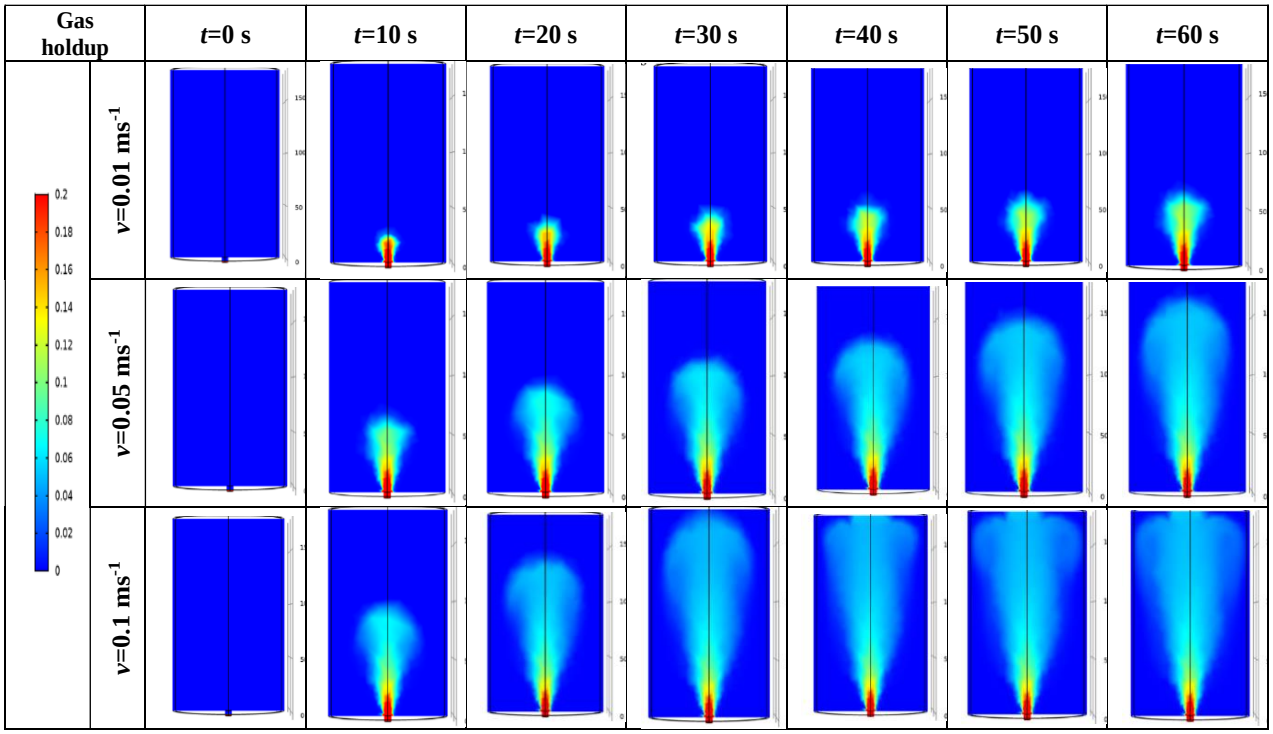

Figure. 7. The gas holdup inside the tank between t=0-60 s at different inlet gas velocity v=0.01, 0.05 and 0.1 ms^{-1}

3.2 Flow Pattern of Gas-Liquid Phase inside a Tank at Different Type of Inlet Gas

Since the type of gas also plays an important role to determine the flow pattern of the gas-liquid phase inside the tank, three types of gases were used as the gas supplied to the tank; carbon dioxide gas, oxygen gas and hydrogen gas. In this case, the inlet gas velocity was fixed at the optimum condition which at v=0.1 ms^{-1}. Figure 8 shows the formation of the gas holdup inside the tank between t=0-60 s at three different types of gas. The bar contour color shows the gas holdup inside the tank where the dark blue color shows the lowest gas holdup; 0 while, the red color shows the highest gas holdup; 0.2. It shows the similar pattern of the formation of gas holdup when the carbon dioxide gas and oxygen gas was supplied to the tank. Yet, for the hydrogen gas, the formation of gas holdup is quite low compared to the others type of gas. It is because the density of hydrogen gas is the lowest as when compared to the density of the carbon dioxide gas and oxygen gas. Besides, it shows the gas holdup is increases as the gas density is increases. This is because as the lower density, the gas will exert a lower momentum forces to develop the bubble formation in the tank [11].

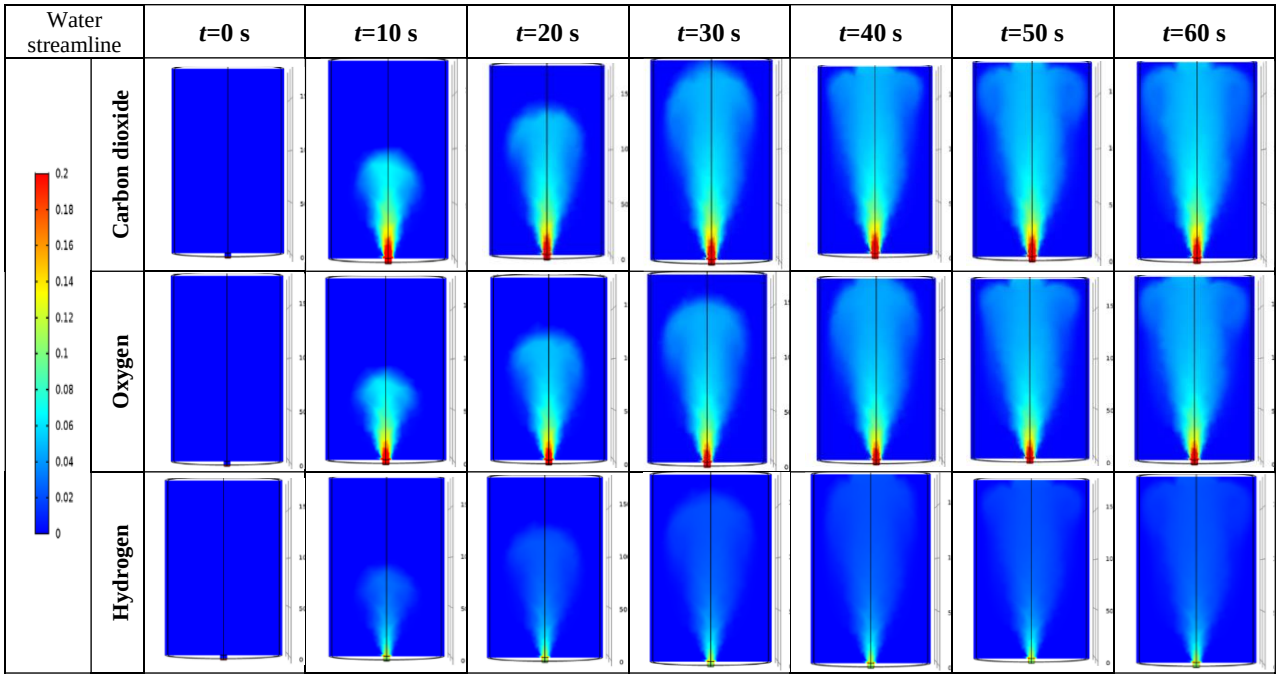

Figure. 8. Gas holdup inside the tank from 0-60 s when feed supplied is a carbon dioxide, oxygen and hydrogen gas.

Figure 9 shows the effect of the type of gas on a gas holdup inside the tank. It was observed that there is no significant pattern difference in the gas holdup as compared between carbon dioxide gas and oxygen gas, although there is marginally difference in a density of carbon dioxide gas which is 40% higher than oxygen gas. But, as the gas density is much lower than 90%, in this case is a hydrogen gas, it shown a clear difference where the maximum gas holdup was achieved at 0.025. This finding is also supported with the studied by Krishna et al. [12] and Hecht et al. [13] where they also found that as the higher of the gas density, the higher of the gas retention was determined.

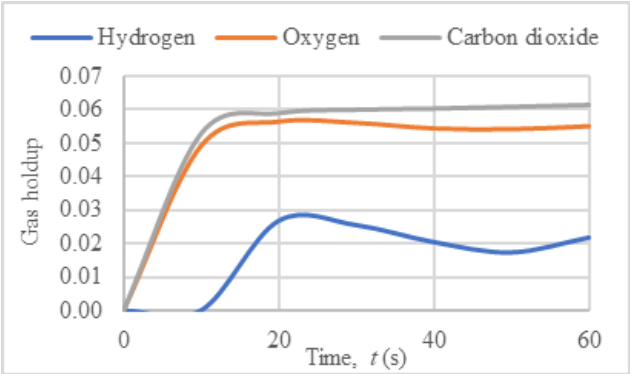

Figure. 9. The effect of type of gas supplied on the gas holdup inside the tank

3.3 The Effect of a Charged Electrode Voltage

The degree of penetration of the electrical field depends on the permittivity of the material inside the flow system [14]. Figure 10 shows the flow profile of the electric field lines when a water and three types of gas were supplied to the tank as the first electrode was charged with E=1-15V, whereas the remaining electrodes (electrode 2-16) were acted as the receivers that obtain a capacitor value correspond to the dielectric in between it [4]. The color contour shows the range of voltage value exerted by the electrode of ECT where the blue color shows the lowest voltage value; 0V and the red color shows the highest voltage value; 4.5V. It shows the electric field lines seem to be reflected as there is a difference on the dielectric permittivity in the tank. It is because the water has a higher dielectric permittivity ($\mathcal{E}_r$=80) as compared to the carbon dioxide gas ($\mathcal{E}_r$=1.6). Besides, the pattern of the electric field from the ECT electrode is similar in case of E=1V, 5V and 15V. It can be concluded that the voltage value on the electric field is increases as the electrode voltage charge is increases. Hitherto, there is no significant difference in the electric field pattern as the similar type of the material was used. It shows the electric field lines tend to bend more around the water due to its

higher dielectric permittivity than the other gases (carbon dioxide gas, oxygen gas and hydrogen gas [14]. However, there is no significant variance when the different type of gases was used as the dielectric permittivity of these three gases is not much dissimilar. Yet, the electric field strength is increases as the electrode voltage charge is increases. Besides, it can be observed that the electric field pattern in the developed ECT model shown the presence of gas in the aeration tank due to the difference in a dielectric permittivity. It can be concluded that the voltage charged on the ECT electrodes not much affected the electric field.

Type of gas	*E*=1V	*E*=5V	*E*=15V
Carbon dioxide	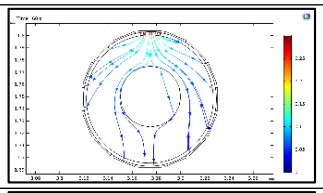	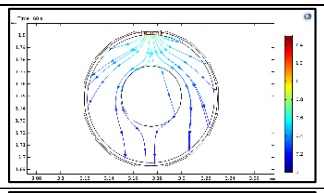	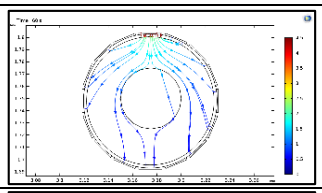
Oxygen	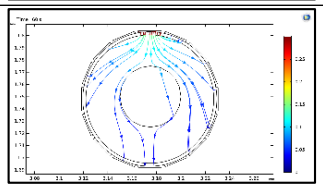	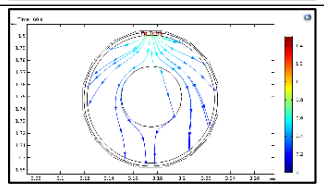	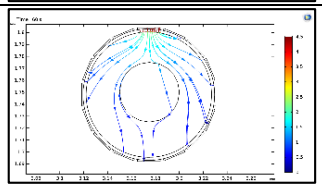
Hydrogen	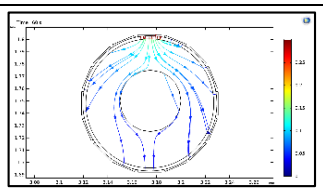	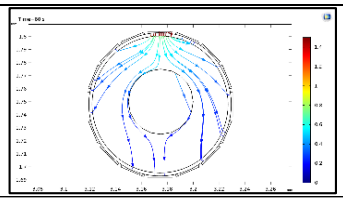	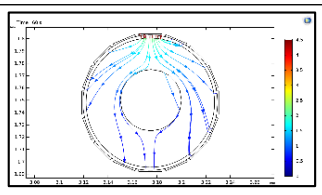

Figure. 10. Electric field lines when water and hydrogen gas were inside the tank at E=1, 5 and 15V

3.4 Determination of Optimum Conditions for Gas-Liquid Phase Flow in Aeration Tank ECT System

The optimum condition of the gas-liquid flow in the aeration tank was determined when the inlet of the gas velocity tend to develop the water turbulence inside the tank throughout the entire tank, while having high gas holdup as the type of gas supplied is capable to achieve higher gas holdup. It is because the gas holdup will determine the degree of interaction and contact between the gas and liquid phases as well it will show an intense interaction between gas and liquid occurs [12]. Figure 11 shows the optimum condition for velocity streamline (a) and optimum gas holdup (b) for the gas-liquid phase flow in the tank at t=60 s. The color of the contour shows the velocity and gas holdup of the gas-liquid phase streamline in the tank where blue color indicates the lowest velocity and gas holdup; 0 ms^{-1} and 0, meanwhile the red color indicates the highest velocity and gas holdup; v=0.01 ms^{-1} and 0.08, respectively.

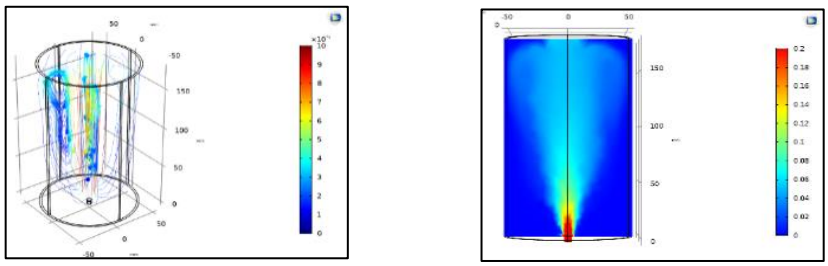

(a) (b)

Figure. 11. The optimum condition for (a) velocity streamline and (b) gas hold-up in gas-liquid phase flow in the tank at t=60 s

Figure 12 shows the optimum condition for averaged water velocity and gas holdup inside the tank at t=60 s. It shows the averaged velocity and gas holdup achieved maximum value at v=0.013 ms^{-1} and 0.059, respectively. Besides, both of the velocity and gas holdup achieved the stable condition after t=30 s that show the development of this ECT model is able to achieve the optimum condition in the shorter time.

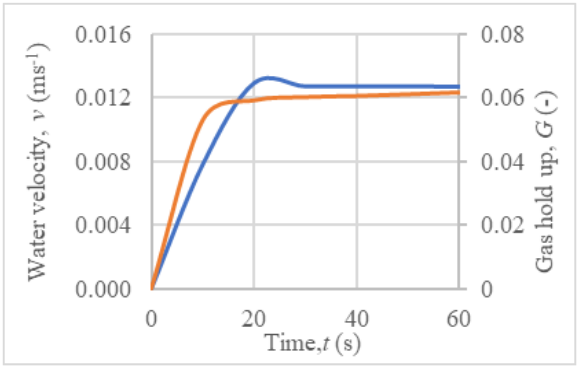

Figure. 12. The optimum average velocity and gas hold-up of gas-liquid phase flow in the tank

4. Conclusion

The ECT model was developed using AutoCAD® 2020 and COMSOL® Multiphysics in order to determine and observe the flow pattern inside the tank. The feed of the hot air velocities between v=0.01-0.1 ms^{-1}, three type of inlet gases (carbon dioxide gas, oxygen gas and hydrogen gas) and electrical charge voltages ranging from E=1-15V were manipulated. The results show the water velocity is increases as the inlet gas velocity is increases as well the gas holdup also increases as the density of gas is increases. In case of different type of gas, gas holdup shown the lowest value when the hydrogen gas was supplied to the tank as compared to others type of gas. In case of the electrical charged at the electrode sensor, there is not much difference as the ECT electrode was charged is quite low which is at E=1V, 5V and 15V. This development of the ECT model can be used for further study for understanding of the multiphase flow state in various industries especially those involving the aeration tanks.

Acknowledgment

The authors would like to thank Universiti Kebangsaan Malaysia for their financial support under the grant GUP-2017-063.

References

[1] Wahab, Y. A., Rahim, R. A., Hafiz Fazlul Rahiman, M., Rahim, H. A., Aw, S. R., Jamaludin, J., & Shima Mohd Fadzil, N. (2014). A review of process tomography application in inspection system. *Jurnal Teknologi, 3*(3), 35–39.

[2] Mohamad, E. J., Rahim, R. A., Leow, P. L., Rahiman, M. H. F., Marwah, O. M. F., & Ayob, N. M. N. (2013). Visualization of recovered palm oil using portable ECT imager in extraction palm oil process. *Flow Measurement and Instrumentation, 31*, 61–68.

[3] Ismail, I., Gamio, J. C., Bukhari, S. F. A., & Yang, W. Q. (2005). Tomography for multi-phase flow measurement in the oil industry. *Flow Measurement and Instrumentation, 16*(2–3), 145–155.

[4] Seong, C. K., Pusppanathan, J., Rahim, R. A., Susiapan, Y. S. L., Phang, F. A., Rahiman, M. H. F., & Aw, S. R. (2015). Mobile electrical capacitance tomography (ECT) development for liquid-gas flow measurement. *Jurnal Teknologi, 73*(3), 29–33.

[5] Chaplin, G., Pugsley, T., Van Der Lee, L., Kantzas, A., & Winters, C. (2005). The dynamic calibration of an electrical capacitance tomography sensor applied to the fluidized bed drying of pharmaceutical granule. *Measurement Science and Technology, 16*(6), 1281–1290.

[6] Marashdeh, Q., Teixeira, F. L., & Fan, L. S. (2015). *Electrical capacitance tomography. In Industrial Tomography: Systems and Applications*.

[7] Peyton, A. J., Yu, Z. Z., Lyon, G., Al-Zeibak, S., Ferreira, J., Velez, J., & Beck, M.S. (1996). An overview of electromagnetic inductance tomography: Description of three different systems. *Measurement Science and Technology, 7*(3), 261–271.

[8] Pendleton, J., & Ladam, Y. (2004). *Visualisation of Two-Phase Gas-Liquid Pipe Flows Using Electrical Capacitance Tomography*. 1–5.

[9] Shafquet, A., Ismail, I., & Jaafar, A. (2014). Modeling and simulation of multi-plane Electrical Capacitance Tomography sensor for flow imaging by using Finite Element Analysis. *2014 5th International Conference on Intelligent and Advanced Systems: Technological Convergence for Sustainable Future, ICIAS 2014 - Proceedings*, 4–9.

[10] Tao, F., Ning, S., Zhang, B., Jin, H., & He, G. (2019). Simulation study on gas holdup of large and small bubbles in a high pressure gas-liquid bubble column. *Processes*, *7*(9).

[11] Kanaris, A., Pavlidis, T., Chatzidafni, A., & Mouza, A. (2018). The Effects of the Properties of Gases on the Design of Bubble Columns Equipped with a Fine Pore Sparger. *ChemEngineering*, *2*(1), 11.

[12] Krishna, R., Wilkinson, P. M., & Van Dierendonck, L. L. (1991). A model for gas holdup in bubble columns incorporating the influence of gas density on flow regime transitions. *Chemical Engineering Science*, *46*(10), 2491–2496.

[13] Hecht, K., Bey, O., Ettmüller, J., Graefen, P., Friehmelt, R., & Nilles, M. (2015). Effect of gas density on gas holdup in bubble columns. *Chemie-Ingenieur-Technik*, *87*(6), 762–772.

[14] Zimam, M. A., Mohamad, E. J., Rahim, R. A., & Ling, L. P. (2011). Sensor modeling for an Electrical Capacitance Tomography system using COMSOL Multiphysics. *Jurnal Teknologi (Sciences and Engineering)*, *55*(2), 33–47.